

## Failure Analysis of Stress Reliever in Heat-Transport Pipe of District Heating System

Jeongmin Cho<sup>1,††</sup>, Hobyung Chae<sup>1,††</sup>, Heesan Kim<sup>2</sup>, Jung-Gu Kim<sup>3</sup>,  
Woo Cheol Kim<sup>4</sup>, and Soo Yeol Lee<sup>1,†</sup>

<sup>1</sup>Department of Materials Science and Engineering, Chungnam National University, Daejeon, 34134, Republic of Korea

<sup>2</sup>Department of Materials Science and Engineering, Hongik University, Sejong 30016, Republic of Korea

<sup>3</sup>School of Advanced Materials Science and Engineering, Sungkyunkwan University, Suwon 16419, Republic of Korea

<sup>4</sup>R&D Institute, Korea District Heating Corp., Yongin 17099, Republic of Korea

(Received June 29, 2022; Revised June 30, 2022; Accepted June 30, 2022)

The objective of the present study was to perform failure analysis of double-layered bellow (expansion joint), a core part of stress reliever, used to relieve axial stresses induced by thermal expansion of heat-transport pipes in a district heating system. The bellow underwent tensile or compressive stresses due to its structure in terms of position. A leaked position suffered a fatigue with a tensile component for decades. A cracked bellow contained a higher fraction of martensitic phase because of manufacturing and usage histories, which induced more brittleness on the component. Inclusions in the inner layer of the bellow acted as a site of stress concentration, from which cracks initiated and then propagated along the hoop direction from the inner surface of the inner layer under fatigue loading conditions. As the crack reached critical thickness, the crack propagated to the outer surface at a higher rate, resulting in leakage of the stress reliever.

**Keywords:** District heating, Heat-transport pipe, Stress reliever, Crack

### 1. Introduction

In developed countries, infrastructures for basic industries were established decades ago. Due to extensive use over a long time, these infrastructures have deteriorated with time, resulting in corrosion and failure. Among various infrastructures, the district heating system contributed significantly to energy production through effective heat production with electric generation in the carbon neutrality era. The demand for these heating systems has increased many folds in the last few decades due to a huge increment in the city population. Unfortunately, numerous failure cases have been reported in the district heating system, resulting in economic losses and highlighting the risks.

The district heating system is composed of units such as heat production, heat transport, and heat usage. The

components of these units are exposed to extreme environments, resulting in various failure patterns. A heat-producing facility such as a boiler is exposed to extreme environments, which induces failure by stress corrosion cracking [1,2], flow accelerated corrosion [3], and localized corrosion [4] of various metallic components. Moreover, failures by stress corrosion cracking of copper pipes for heat supply in a heat usage facility were also reported [5]. The most critical unit of the district heating system is the heat transport unit, as it is installed downtown, and its integrity is directly related to the safety of citizens. As the components of the heat transportation unit are installed underground, it is difficult to manage and observe its degradation directly. Corrosion cases caused by lagging materials [6,7] and localized corrosion caused by pipe inclusion [8] have been reported in heat-transport pipes observed through a manhole. However, the number of these reports is insufficient compared to their importance. Failure in the district heating system results in an economic loss by suspension of operation, casualties by leakage of heat transport pipe at urban core, and inconvenience of citizens by a service failure. Thus,

<sup>†</sup>Corresponding author: [sylee2012@cnu.ac.kr](mailto:sylee2012@cnu.ac.kr)

<sup>††</sup>These authors contributed equally: J. Cho, H. Chae  
Jeongmin Cho: Researcher, Hobyung Chae: Researcher, Heesan Kim: Professor, Jung-Gu Kim: Professor, Woo Cheol Kim: Senior researcher, Soo Yeol Lee: Professor

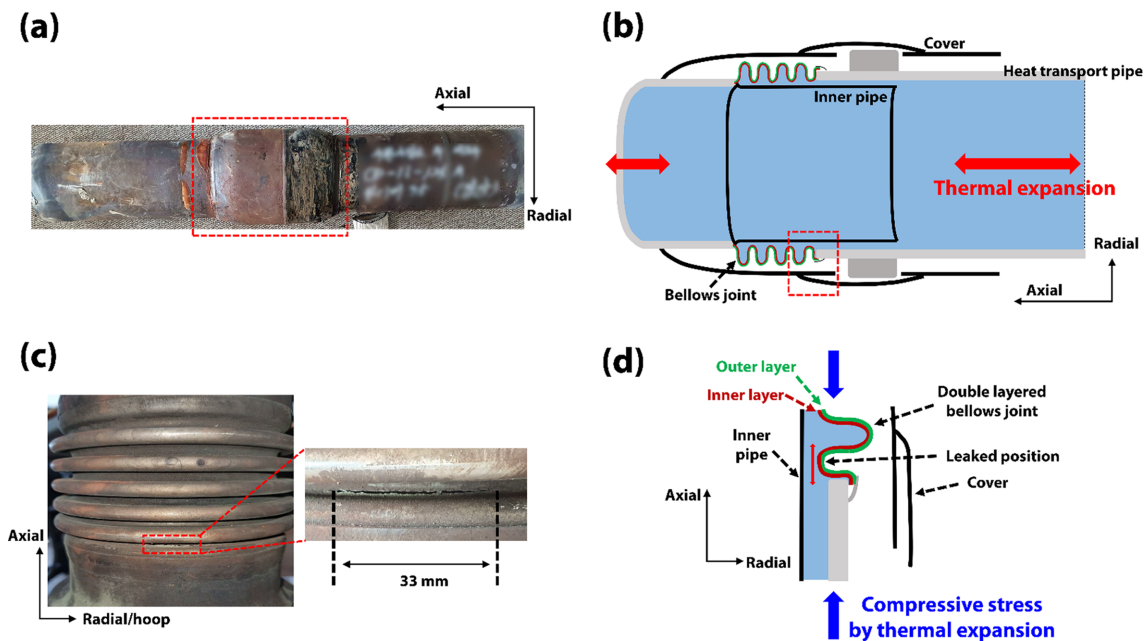


**Fig. 1.** (a) Leaked stress reliever installed with heat-transport pipes, (b) schematics of a cross-section of stress-reliever indicated by the red dash-line box shown in (a), (c) images of cracked bellows joint and its crack, (d) schematics of bellows joint indicated by the red dash-line box shown in (b).

reporting the failure cases and methodology for establishing countermeasures and preventive measures needs to be more emphasized.

The present study deals with leakage of stress reliever for relieving the stress of pipes induced by thermal expansion in heat-transport infrastructure. The stress reliever indicated by the red box in Fig. 1a is located between heat transport pipes of 125 mm in diameter. It is exposed to corrosive environments such as 0 ~ 120 °C and 16 bar of pressure from hot water, which induces thermal expansion and/or contraction of pipes. During operation, these axial stresses of pipes are relieved by shrinking or stretching the bellows joint (Fig. 1b). It is usually installed and used at specific distances. In this study, the leakage test was performed on the pipes assembled with the stress reliever, and the leakage between heat-transport pipes and the cover was observed (Fig. 1a) by disassembling it. A crack of 33 mm length along the hoop direction on the lower part of the bellows joint was found, and heat transport water was leaked through it (Fig. 1c).

A visual inspection to identify leakage patterns was performed to determine the cause of stress reliever leakage in heat-transport infrastructure that has been in use for over 25 years. Further, comparing cracked bellows joint

with crack-free counterpart using microstructural and fractographical analyses was carried out to determine the failure mechanism. The results of the present study will also pave the way for industries and academia that require corrosion failure analysis.

## 2. Experimental methods

SPPS380 and stainless steel 304/304L are used for heat-transport pipe and bellows joint, respectively (Table 1). The structure of the stress reliever was presented in Fig. 1b, which exhibits that the double-layered bellows joint can easily experience compression-compression fatigue by thermal expansion of heat-transport pipes on both sides. The leakage position of the bellows joint was indicated by the red box in Fig. 1b, which was then magnified in Fig. 1d. It comprises two layers with 0.4 mm thickness each, and the inner and outer layers are marked by red and green colors (Figs. 1b, 1d). Fig. 1c shows the location of a 33 mm-long crack along the hoop direction, which corresponds to the valley closest to the heat-transport pipe. It was further estimated that the inside of this valley should be subjected to tensile stress when both sides of heat-transport pipes compressed the bellows joint.

**Table 1. Nominal chemical composition of heat-transport pipe and bellows joint (wt%)**

Component	Type	Fe	Cr	Ni	Mn	C	Si	P	S
Heat-transport pipe	SPPS380	Bal.	-	-	0.3-1.0	~0.3	~0.35	~0.04	~0.04
Bellows joint	SS304	Bal.	18.0-20.0	8.0-10.5	~2.0	~0.08	~1.0	~0.045	~0.03
	SS304L	Bal.	18.0-20.0	9.0-13.0	~2.0	~0.03	~1.0	~0.045	~0.03

To understand the causes of cracking, a working stress reliever installed at an identical site was collected and compared with the failed stress reliever. Since only small amounts of corrosion products were deposited on the surface of the bellows joint without extreme damage by corrosion, it was expected that mechanical factors should be responsible for this failure. To compare the precise chemical composition and phase constituent of bellows joints in both stress relievers, inductively coupled plasma-atomic emission spectroscopy (ICP-AES) and X-ray diffraction (XRD) were used. Quantitative information of phase constituents in the XRD spectrum was calculated

by Rietveld refinement. Cracking behaviors were then defined by observation of inner/outer/fracture surfaces of the cracked bellow joint using optical microscopy (OM) and scanning electron microscopy (SEM) with electron backscatter diffraction (EBSD).

### 3. Results

#### 3.1. Bellows joints

Leakage was observed at only one stress reliever, although both stress relievers were installed in similar environments and were used for a similar period. Thus,

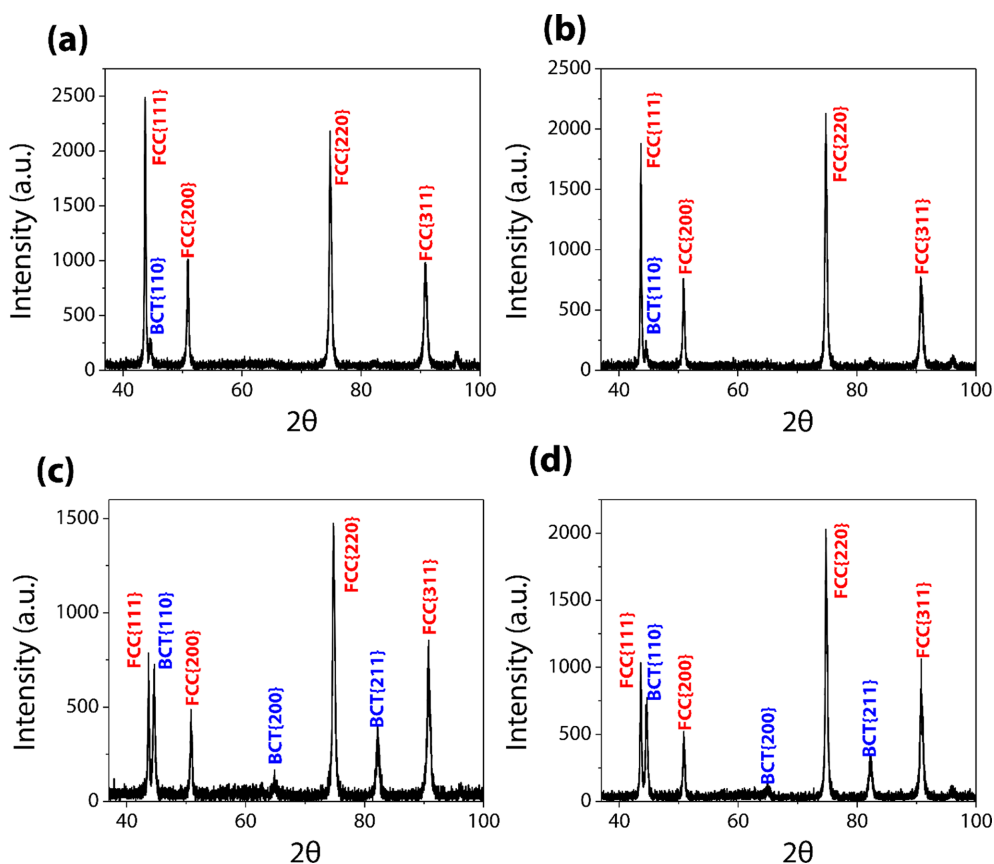


**Fig. 2. X-ray diffraction spectra for (a) inner and (b) outer layers of crack-free bellows joint, and (c) inner and (d) outer layers of cracked bellows joint**

their chemical composition and phase constituents were compared to unravel the difference between both bellows joints. The chemical composition of the crack-free and cracked bellows joints measured by ICP-AES was presented in Table 2. While the chemical composition of outer and inner layers in both bellows joints was almost similar, a slight difference between crack-free and cracked bellows joints was observed. It is not directly related to cracking, but it can be speculated that the manufacturing history of each bellows joint was different. Fig. 2 shows XRD results of the crack-free and cracked bellows joints, which revealed that both components contained a face-centered cubic (FCC) austenitic phase for the matrix and body-centered tetragonal (BCT) martensitic phase. Phase constituents were obtained by Rietveld refinement on diffraction spectra, which exhibited that the contents of martensitic phase in the inner and outer layers of the crack-free bellows joint were 5.6% and 4.2%, and those of the cracked counterpart were 31.3% and 30.4%, respectively. The higher fraction of the martensitic phase in the cracked bellows joint induces more brittleness in the component, which can assist initiation and propagation of cracking.

**3.2. Cracking behavior and inclusions**

Cracking behavior reflects on the causes and history of failure. Fig. 3 shows the secondary cracks of inner and outer layers near the tip of the main crack. It can be observed that numerous secondary cracks were found along the hoop direction on the inner surface of the inner layer (Fig. 3a), while a relatively lower number of secondary cracks was discovered on the outer surface of the inner layer (Fig. 3b). Similar trends were observed in the outer layer, where more secondary cracks were revealed on the inner surface than on the outer surface in the outer layer (Figs. 3c, 3d). These indicate that the cracks were initiated from the inner surface of both double layers in the bellows joint.

Figs. 4a and 4b present that the secondary cracks in the inner surface of the inner layer propagated with a transgranular mode, which exhibits the brittle fracture behavior of the austenitic matrix [9]. The history of the cracking behavior is inferred from the morphology of the fracture surfaces. A distinct beach mark lay on the fracture surface close to the inner surface (Fig. 4c), which indicates that through-thickness-direction cracking behavior was changed during crack propagation. In particular, several ratchet marks on the inner surface side of the fracture

**Table 2. Chemical composition of crack-free and cracked bellows joints obtained by ICP-AES (wt%)**

Bellows joint	Layer	Fe	Cr	Ni	Mn	Si	P	S
Crack-free	Inner	71.46	17.18	9.08	1.42	0.23	<0.01	<0.01
	Outer	71.65	17.02	9.01	1.62	0.28	<0.01	<0.01
Cracked	Inner	72.22	16.61	8.81	1.35	0.27	<0.01	<0.01
	Outer	71.79	16.72	8.81	1.43	0.29	<0.01	<0.01

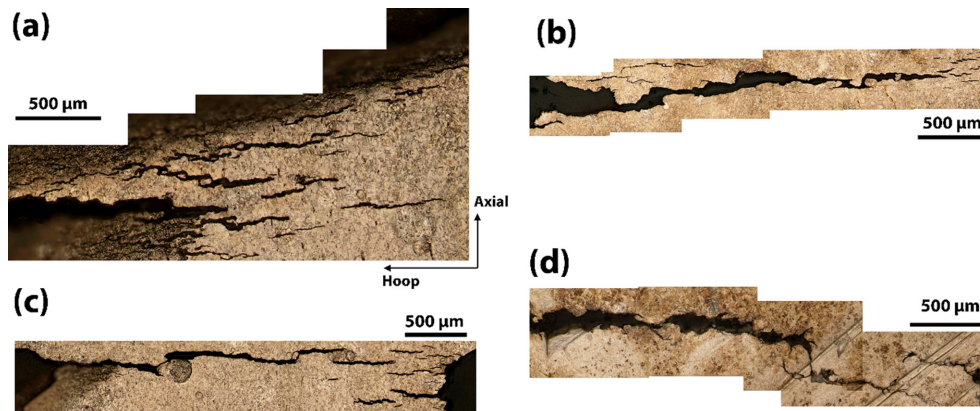


**Fig. 3. OM images of the secondary cracks near the main crack and its tip on (a) inner and (b) outer surfaces of the inner layer, and (c) inner and (d) outer surfaces of the outer layer**

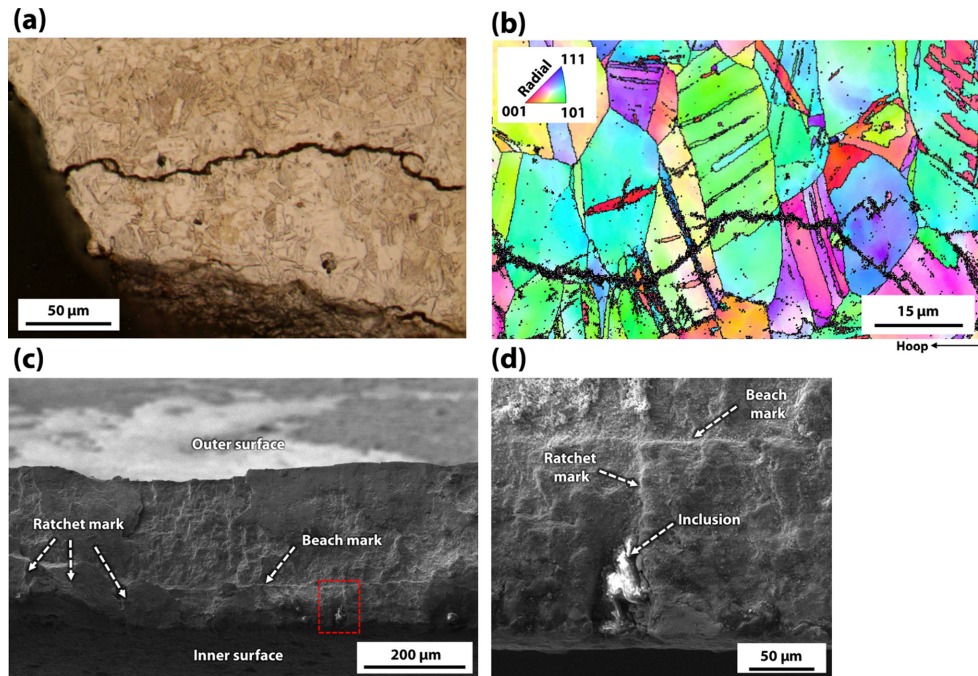


Fig. 4. (a) OM image, (b) inverse pole figure map showing the propagation of the secondary crack on the inner surface of the inner layer, (c) fracture surface of the inner layer, and (d) magnified area of red-dashed line box shown in (c)

Table 3. EDS measurement of the chemical composition of the inclusion shown in Fig. 4d (at.%)

O	C	Cr	Fe	Ca	etc.
38.1	24.1	14.2	11.2	7.8	Mg, Ti, Si, Mn, Cl, K, S, Na

surface indicate that crack initiation points were located on the inner surface side of the layer. A magnified Fig. 4d shows the inclusion, ratchet mark, and beach marks. The chemical composition of the inclusions is presented in Table 3. It is difficult to define it precisely, but it might be the oxide which has been generated or not removed during the manufacturing process [10]. Since it was embedded near the inner surface of the inner layer, external load by thermal fatigue should be concentrated in the vicinity of these inclusions.

#### 4. Discussion

Damages near the cracks of bellow joints caused by corrosion such as pit, which is critical to stainless steel, were not observed. This indicates that environmental corrosive factors hardly contributed to the failure. On the other hand, the higher fraction martensitic phase in the cracked bellows joint has imposed higher strength and brittleness. Thus, the crack was easily created and

propagated at a relatively higher rate. ICP-AES results revealed that the manufacturing history of both crack-free and cracked bellows joints was slightly different, however, both components were exposed to identical environments. Therefore, we can anticipate that the cracked component contained a more martensitic phase before installation, or it was in the condition where transformation-induced plasticity (TRIP) could be activated by an external load due to the difference in manufacturing history between both components. Consequently, higher contents of the martensitic harder phase in the cracked component led to relatively easier onset and propagation of cracking.

A thermal gradient of heat-transport pipes induced by the flow of hot water made the pipes be axially extended (Fig. 1b), which imposed compressive stresses on the bellows joints (Fig. 1d). Due to the structure of the bellows joint, it should induce axial tensile stress on the inner surface which is a leakage position and weak axial tensile or compressive stresses on the outer surface. Thus, stress relievers with heat-transport pipes experienced the repetitive

stress field during operation for a long time. Furthermore, the inner surface underwent a fatigue with an axial tensile component. This was the driving force to generate a TRIP of austenitic phase in bellows joint and to propagate along with hoop and through-thickness directions.

It is thought that the crack was initiated from the inclusion, as shown in Figs. 4c and 4d, because the inclusion is a site as a stress concentration under the fatigue during operation. The cracks initiated from the vicinity of the inclusion left a ratchet mark as a result of crack propagation on the fracture surface (Fig. 4d), and other onsets of cracks also created ratchet marks on their sites (Fig. 4c). The beach mark close to the inner surface of the fracture surface indicates that the crack propagation rate was different between the upside and downside of the beach mark. In other words, the crack was initiated from the inner surface of the inner layer, and it was propagated along the hoop and through-thickness directions until the tip of the cracks reached a beach mark. Then, the crack propagation reached a critical thickness (beach mark thickness), in which the bellows joint could no longer withstand, thus the crack propagated to the outer surface at a higher speed.

## 5. Conclusions

Failure analysis of stress relievers in a heat-transport pipe of a district heating system was conducted. The following conclusions are drawn:

Stress relievers located in heat transport pipes experienced the repetitive stress during operation, as confirmed by the observation of ratchet mark and beach mark in fractography.

The inclusion induced the crack initiation due to its stress concentration effect under the fatigue condition. The cracks initiated from the inner surface of inner layer have propagated along the hoop and through-thickness directions until the tip of the cracks reached critical thickness close to the beach mark.

For countermeasures and preventive measures, the process to verify the identical or uniform quality of the bellow joint and its material is required. Since it experiences continuous fatigue, the materials exhibiting stable TRIP performance are recommended. Inclusions in stainless steel should be avoidable and managed.

## Acknowledgment

This work was supported by the research funds of Korea District Heating Corporation.

## References

1. M. Hong, H. Chae, W.C. Kim, J.-G. Kim, H. Kim, and S.Y. Lee, Failure analysis of a water wall boiler tube for power generation in a district heating system, *Metals and Materials International*, **25**, 1191 (2019). Doi: <https://doi.org/10.1007/s12540-019-00267-6>
2. H. Chae, W.C. Kim, H. Kim, J.-G. Kim, K.M. Kim, and S.Y. Lee, Corrosion failure analysis of condensate pre-heater in heat recovery steam generator, *Corrosion Science and Technology*, **20**, 69 (2021). Doi: <https://doi.org/10.14773/CST.2021.20.2.69>
3. M. Hong, H. Chae, Y. Kim, M.J. Song, J. Cho, W.C. Kim, T.B. Ha, and S.Y. Lee, Flow-accelerated corrosion analysis for heat recovery steam generator in district heating system, *Korean Journal of Materials Research*, **29**, 11 (2019). Doi: <https://doi.org/10.3740/MRSK.2019.29.1.11>
4. Y. Kim, H. Chae, M. Hong, M.J. Song, J. Cho, S.Y. Lee, W.C. Kim, and T.B. Ha, Corrosion failure analysis of the convection part of district heating peak load boiler, *Corrosion Science Technology*, **18**, 55 (2019). Doi: <https://doi.org/10.14773/cst.2019.18.2.55>
5. H. Chae, H. Wang, M. Hong, W.C. Kim, J.-G. Kim, H. Kim, and S.Y. Lee, Stress corrosion cracking of a copper pipe in a heating water supply system, *Metals and Materials International*, **26**, 989 (2019). Doi: <https://doi.org/10.1007/s12540-019-00386-0>
6. H. Lee, H. Chae, J. Cho, W.C. Kim, J.C. Jeong, H. Kim, J.-G. Kim, and S.Y. Lee, Corrosion failure analysis of air vents installed at heat transport pipe in district heating system, *Corrosion Science and Technology*, **19**, 189 (2020). Doi: <https://doi.org/10.14773/CST.2020.19.4.189>
7. J. Cho, H. Chae, H. Kim, J.-G. Kim, W.C. Kim, J.C. Jeong, and S.Y. Lee, Failure analysis of air vent connected with heat supply pipeline under manhole, *Corrosion Science and Technology*, **19**, 196 (2020). Doi: <https://doi.org/10.14773/CST.2020.19.4.196>
8. Y.S. Kim, H. Chae, W.C. Kim, J.C. Jeong, H. Kim, J.-G. Kim, and S.Y. Lee, Failure analysis on localized corrosion of heat transport pipe in district heating system, *Corrosion Science and Technology*, **19**, 122 (2020). Doi: <https://doi.org/10.14773/cst.2020.19.3.122>

9. T.L. Anderson, Fracture mechanics: fundamentals and applications, CRC Press (2017).
10. H. Todoroki, K. Mizuno, Variation of inclusion composition in 304 stainless steel deoxidized with aluminum, *Iron and Steelmaker*, **30**, 60 (2003).